LASER SPECTROSCOPY

PACS numbers: 42.62.Fi; 42.62.Eh; 33.15.Pw
DOI: 10.1070/QE2008v038n08ABEH013761

Study of the hyperfine structure of emission lines of I_2 molecules by the method of three-level laser spectroscopy

Yu.A. Matyugin, M.V. Okhapkin, M.N. Skvortsov, S.M. Ignatovich, S.N. Bagayev

Abstract*. It is proposed to use narrow optical resonances, corresponding to the hyperfine structure components of emission transitions in I_2, as frequency references to stabilise laser radiation frequency in the spectral range from 0.8 to 1.3 μm. To obtain such resonances and investigate the hyperfine structure of emission transitions, an experimental setup is built which consists of a saturated absorption laser spectrometer and a three-level laser spectrometer. Excitation is performed by the second harmonic of a cw Nd : YAG laser and probe radiation in the range from 968 to 998 nm is generated by an external cavity diode laser. The radiation beams from both lasers are combined in a cell with iodine vapour, excitation in the cell being performed in the regime of two counterpropagating waves. It is shown that upon phase modulation of exciting radiation, narrow resonances, having the form of the dispersion dependence, appear at the centre of Doppler lines in absorption and emission. These resonances can be used as references to stabilise the laser frequency. The results of the study of the hyperfine structure of emission lines at the $(J' = 57, v' = 32) \rightarrow (J'' = 58, v'' = 48)$ transition upon excitation at the $(J'' = 56, v'' = 0) \rightarrow (J' = 57, v' = 32)$ transition are presented.

Keywords: *iodine spectroscopy, three-level laser spectroscopy, Nd : YAG laser, external cavity diode laser, laser frequency stabilisation.*

1. Introduction

At present the absorption lines of molecular iodine are widely used as frequency references in the spectral range between 500 and 650 nm. By heating iodine vapour, the absorption spectrum can be extended up to 900 nm due to the population of high vibrational – rotational levels of the ground electronic state. In this case, the absorption spectrum contains about 100000 discrete lines. The absorption spectra of iodine and tabulated wave numbers for strong absorption lines are presented in atlases [1]. The absorption lines of iodine have the asymmetric contour of width ~ 1500 Hz and their shape is determined by the superposition of hyperfine structure (HFS) components, which are unresolved due to the Doppler broadening. The centres of lines in atlases [1] are determined with the relative error $\sim 3 \times 10^{-7}$. A higher accuracy can be achieved by using as frequency references the HFS components which can be resolved by the methods of laser saturation spectroscopy. In this case, individual components have the form of narrow (~ 1 MHz) optical resonances (15 or 21 resonances) lying within a region of width ~ 1 GHz. Thus, taking into account HFS components, the absorption spectrum of iodine contains $\sim 10^6$ frequency references in the spectral range from 500 to 900 nm.

Saturated absorption resonances are excellent references for laser frequency stabilisation. The accuracy of locking to the resonance centre achieves 10^{-14} and the frequency reproducibility is 10^{-13}. A number of lasers stabilised by the HFS components of iodine were recommended as length and frequency standards.

During the past decade, systematic precision measurements of the frequencies of individual HFS components in the absorption spectrum of iodine have been performed. The frequencies of several thousands of lines were measured in the range from 526 to 667 nm with an accuracy of 1 – 3 MHz [2 – 5]. By using the frequency synthesis method, the frequencies of HFS components of two lines were measured in the near-IR range from 729 to 732 nm with an accuracy of $\sim 10^{-9}$ [6, 7] and systematic measurements were performed in the range from 776 to 815 nm with an accuracy of 4×10^{-11} [8 – 10]. Even more accurate measurements ($\sim 10^{-12}$) were performed for a number of lines in the 532-nm region by using a femtosecond synthesiser [11 – 13]. The results of all these measurements were systematised in papers [14, 15] and used to refine the spectroscopic parameters of iodine molecules. Interpolation expressions were also obtained which were used to calculate the frequencies of individual HFS components with an accuracy of no worse than 3 MHz in the spectral range from 526 to 667 nm and no worse than 200 kHz in the range from 778 to 815 nm. Thus, the accuracy of the frequency scale represented by the absorption spectrum of iodine was improved by one – two orders of magnitude in a broad spectral range in recent years.

In our opinion, it is important not only to further improve the accuracy of the frequency scale over the entire absorption spectrum but also to extend this scale to the red – to the emission spectrum region extending up to 1.35 μm. Narrow resonances in the emission spectrum can be

Yu.A. Matyugin, M.V. Okhapkin, M.N. Skvortsov, S.M. Ignatovich, S.N. Bagayev Institute of Laser Physics, Siberian Branch, Russian Academy of Sciences, prosp. akad. Lavrent'eva 13/3, 630090 Novosibirsk, Russia; e-mail: matyugin@laser.nsc.ru, maxok@laser.nsc.ru, skv@laser.nsc.ru, bagaev@ilph.nsk.su

Received 21 November 2007
Kvantovaya Elektronika **38** (8) 755 – 763 (2008)
Translated by M.N. Sapozhnikov

obtained by exciting iodine molecules by a single-frequency laser. In this case, iodine molecules are excited on the upper level in a very narrow velocity range, and a narrow amplification peak of width of the order of the homogeneous linewidth appears. Transitions from the excited level can occur to any of the 108 vibrational levels of the ground X state. If the excitation power is high enough, lasing can be obtained at these transitions. This circumstance was used first of all to study resonances.

Optically pumped I_2 lasers have been studied in many papers [16–23]. Iodine molecules were excited by argon [17–19] and krypton [21] lasers, a cw dye laser [20], and second harmonics of pulsed [16] and cw [22, 23] Nd : YAG lasers. In these papers, a very narrow amplification line was observed in the emission spectra of I_2 lasers and it was pointed out [19, 23] that optically pumped I_2 lasers can be used as optical frequency standards. However, no precision measurements of transition frequencies in the emission spectrum were performed. The hyperfine structure of emission lines also was not investigated in a broad range of vibrational and rotational quantum numbers. In our opinion, this is explained by the fact that pump lasers used in these papers were not suitable for such studies.

To obtain frequency references with the high frequency reproducibility, pump lasers should have themselves parameters typical for frequency standards because the central frequency of the frequency reference is determined by the pump frequency. In addition, to obtain a dense comb of frequency references, it is necessary to excite many transitions and, therefore, the pump laser should be tunable in a broad spectral range. Finally, to obtain lasing, the output power of the pump laser should be high. Lasers used in the papers mentioned above did not have such parameters.

Recently the situation with pump lasers has changed considerably. Compact, simple, and reliable diode-pumped frequency-doubled lasers were developed. By locking the second harmonic of such lasers to absorption resonances in iodine molecules, frequency standards were created [24, 25]. In this case, along with the high frequency stability, a broad tuning range of the laser was achieved [25]. The use of a Nd : YAG standard for pumping an iodine laser was demonstrated in paper [23]. It was shown that it was possible to achieve the frequency stability of the iodine laser at the level of 10^{-10}.

The use of lasing for studying narrow amplification lines has the advantage because it allows the study of emission transitions in a broad spectral range without employing additional lasers. At the same time, we believe that the direct investigation of narrow resonances by the method of three-level laser spectroscopy [26], i.e. by probing the adjacent transition with the help of an additional laser offers a number of advantages. First, this reduces the requirements on the pump laser power, i.e. a simpler and cheaper laser can be used for pumping. Second, the number of transitions suitable for investigation considerably increases and the spectral range covered by them broadens. This is explained by the fact that weaker transitions can be studied additionally, as well as transitions for which the lower levels are populated and, as a result, the gain is insufficient to obtain lasing.

The method of three-level laser spectroscopy was applied earlier for studying narrow resonances in iodine molecules in paper [27], where probing was performed by using a tunable dye laser. However, investigations in this direction were not further developed. In our opinion, this is mainly explained by the fact that resonances obtained in this spectrometer lie in the visible range and are of little interest as frequency references because absorption saturation resonances can be considerably simpler obtained in this range. Suitable lasers tunable in the 0.9 – 1.3-μm range were absent at that time. At present there exist simple and available semiconductor lasers which can be tuned almost within this entire range. A combination of an efficient pump Nd : YAG laser with a probe semiconductor laser opens up excellent possibilities for studying optical resonances in the emission spectrum of iodine molecules.

In this paper, we describe a laser spectrometer for the three-level spectroscopy of molecular iodine. The spectrometer is intended for studying stimulated emission resonances and estimating the applicability of these resonances to stabilise laser frequencies.

2. Description of the method

In the method of three-level laser spectroscopy [26], two laser fields interact simultaneously and resonantly with two adjacent transitions having the common upper level. The radiation of one of the lasers tuned to the absorption line of iodine is absorbed in a cell with iodine vapour by exciting iodine molecules from the ground X state to the electronic B state (Fig. 1), from which transitions can occur to any vibrational level of the ground state. The radiation of the second probe laser tuned to the frequency of such a transition is spatially combined with radiation from the first laser and, passing through the cell, interacts with molecules excited by the first laser. Because molecules are excited in a narrow velocity interval, the second laser detects a narrow amplification peak during tuning. If the exciting field frequency is tuned exactly to the centre of the Doppler absorption line, the peak at the adjacent transition will also correspond to the centre of the adjacent transition frequency.

The interaction of two optical fields with a resonance three-level system was studied in many papers (see reviews [26, 28]). One of the specific features of resonances appearing in the three-level system is their anisotropy. The resonance frequency and its shape depend on the mutual

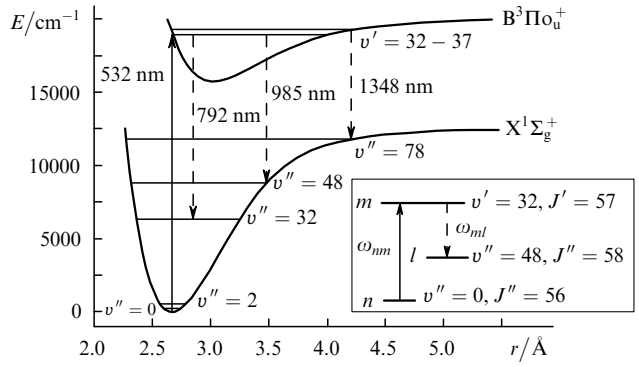

Figure 1. Potential-energy curves for the X and B levels of the I_2 molecule. In the tuning range of the Nd : YAG laser, the vibrational levels of the B state with $\upsilon' = 32 - 37$ can be excited. From these levels, transitions can occur to the vibrational levels of the ground electronic states with $\upsilon'' = 2 - 78$ in the range from 534 to 1348 nm. The inset shows the levels of transitions studied in the paper.

direction of interacting fields. In the general case the resonances have a rather complex shape, which is determined by one-photon and two-photon processes. The shape of resonances in intense pump fields strongly depends on the dynamic Stark effect. This effect broadens the resonance, and a dip is formed at the resonance centre in high-power pump fields or even complete splitting of the resonance can occur.

In the first approximation in weak pump fields, the shape of resonances is close to Lorentzian. The FWHM of resonances for copropagating (Γ^+) and counterpropagating (Γ^-) waves are [26]

$$\Gamma^+ = \gamma_n + \gamma_l + \left(1 - \frac{k}{k_\mathrm{p}}\right)\gamma_m, \tag{1}$$

$$\Gamma^- = \gamma_n + \gamma_l + \left(1 + \frac{k}{k_\mathrm{p}}\right)\gamma_m, \tag{2}$$

where γ_i are the relaxation constants of levels and k_p and k are the wave numbers of the pump and probe fields, respectively. In the case of a small difference between the pump and probe radiation wavelengths, i.e. when $k \approx k_\mathrm{p}$, the resonance width for copropagating waves is equal to the forbidden transition width, $\Gamma_{nl} = \gamma_n + \gamma_l$. The line narrowing in the case of copropagating waves is caused by the compensation of the Doppler shift during the two-quantum $n \to m \to l$ transition.

If the pump frequency ω_p is shifted with respect to the Doppler line centre ω_{mn}, molecules are excited in the vicinity of the velocity v determined by the relation $\omega_n = \omega_{nm} \pm k_\mathrm{p} v$. The plus sign corresponds to the case when the wave vector direction coincides with the direction of the velocity projection of the molecule. In this case, the velocity is

$$v = \frac{1}{k_\mathrm{p}}(\omega_\mathrm{p} - \omega_{nm}). \tag{3}$$

The frequency of the resonance interaction of excited molecules with the probe wave depends on the direction of its propagation. For the probe wave propagating in the same direction as the pump wave, this frequency is

$$\omega^+ = \omega_{ml} + \frac{k}{k_\mathrm{p}}(\omega_\mathrm{p} - \omega_{nm}), \tag{4}$$

for the wave propagating in the opposite direction, this frequency is

$$\omega^- = \omega_{ml} - \frac{k}{k_\mathrm{p}}(\omega_\mathrm{p} - \omega_{nm}). \tag{5}$$

This circumstance plays a decisive role in the analysis of the HFS spectrum recorded at the emission transition.

The HFS components are distributed within the absorption line in the interval from 860 to 900 MHz and the FWHM of the Doppler contour of an individual component at 530 nm is approximately 260 MHz at $T = 300$ K. Because of this almost all the lines are overlapped and the pump radiation interacts with molecules corresponding to all overlapped lines. As a result, for HFS components with different frequencies ω_{nm}, molecules with different velocities determined by relation (3) are excited, and each of these molecular groups will emit at the adjacent transition according to (4) and (5) at its own frequency determined by its own Doppler shift. Thus, although all the HFS components of the absorption line interact with the same frequency, we can obtain emission containing almost all the HFS spectrum of the emission line.

Unlike the saturated absorption method, when the entire HFS spectrum can be recorded at once during laser tuning, three-level spectroscopy detects only HFS components for which the upper levels are excited at the given moment by the pump laser. The number of excited components and intensity of resonances depend on the position of the pump frequency within the absorption line. If the detuning of the pump frequency from the centre of the Doppler profile of some component considerably exceeds the Doppler profile width, molecules of such components are not excited and, hence, resonances are not recorded.

The hyperfine structure is usually studied by measuring frequency intervals between resonances. The HFS components within a line are denoted, as a rule, by ordinal numbers increasing with increasing frequency. To obtain relations convenient for spectral analysis, consider two overlapping Doppler profiles corresponding to two components of a HFS absorption line at frequencies ω_1 and ω_2, to which the centres of Doppler profiles correspond. Each of these two transitions is related to the emission transition coupled to it through the common upper level. Denote the frequencies of these emission transitions by Ω_1 and Ω_2. Let the pump frequency be coincident with the transition frequency ω_1 ($\omega_\mathrm{p} = \omega_1$) and $\omega_1 < \omega_2$. According to (3), molecules with velocities v_1 are excited in the first contour and molecules with velocities $v_2 = k_\mathrm{p}^{-1}(\omega_1 - \omega_2)$ – in the second contour. Let us find resonance frequencies at coupled transitions by using relations (4) and (5), taking into accounts that $\omega_1 < \omega_2$. We obtain

$$\Omega_1^+ = \Omega_1, \quad \Omega_2^+ = \Omega_2 - \frac{k_\mathrm{e}}{k_\mathrm{p}}(\omega_2 - \omega_1), \tag{6}$$

$$\Omega_1^- = \Omega_1, \quad \Omega_2^- = \Omega_2 + \frac{k_\mathrm{e}}{k_\mathrm{a}}(\omega_2 - \omega_1). \tag{7}$$

Here, k_a and k_e are the wave numbers of the centres of absorption and emission lines, respectively. Strictly speaking, it is necessary to use in (6) and (7) the wave numbers of the fields corresponding to each of the recorded resonances. However, the values of these numbers taken from a handbook or calculated correspond to the centres of the lines and, in addition, the accuracy of their measurement is the same or even worse than the accuracy of measurements of frequency intervals between the components. Therefore, we assume in the first approximation that the ratio of wave numbers is constant for all the HFS components. Taking this into account, we find the values of frequency intervals from relations (6) and (7):

$$\Delta\Omega_{21}^+ = \Omega_2^+ - \Omega_1^+ = \Delta\Omega_{21} - \frac{k_\mathrm{e}}{k_\mathrm{a}}\Delta\omega_{21}, \tag{8}$$

$$\Delta\Omega_{21}^- = \Omega_2^- - \Omega_1^- = \Delta\Omega_{21} + \frac{k_\mathrm{e}}{k_\mathrm{a}}\Delta\omega_{21}, \tag{9}$$

where $\Delta\Omega_{21} = \Omega_2 - \Omega_1$ and $\Delta\omega = \omega_2 - \omega_1$.

Thus, if the HFS of the absorption line is known (i.e. frequency intervals between components of the line are

known), we can calculate frequency intervals between components of the emission line by using the measured intervals between resonances for counterpropagating and copropagating waves. By using (8) and (9), we obtain the expressions

$$\Delta\Omega_{21}^{-} - \Delta\Omega_{21}^{+} = 2\,\frac{k_e}{k_a}\,\Delta\omega_{21}, \tag{10}$$

$$\Delta\Omega_{21} = \frac{1}{2}(\Omega_{21}^{+} + \Delta\Omega_{21}^{-}), \tag{11}$$

which can be used to analyse the HFS spectra. If resonances for copropagating and counterpropagating waves are recorded together in a spectrogram and the frequency scale is defined in arbitrary units, for example, in the units of voltage across a piezoelectric element or in the length units, we can find from (10) the frequency scale and absolute values of frequency intervals between resonances. By using (11), we can calculate the frequency interval between HFS components for the emission transition.

3. Experimental setup

The pump source in our spectrometer was a diode-pumped Nd : YAG laser with intracavity frequency conversion, which we developed earlier [25]. The ring cavity of the laser provided single-frequency unidirectional travelling wave lasing. The second harmonic was generated in an intracavity KTP crystal with the optical axis oriented at an angle of 45° to the direction of polarisation of fundamental radiation in the cavity. The KTP crystal in this orientation can be used as a birefringent optical element forming together with a polariser a frequency-selective Lyot filter. An active element with one of the end-faces cut at the Brewster angle plays the role of the polariser. The laser could be tuned in a broad spectral range by varying the KTP crystal temperature. The tuning range for the fundamental radiation depends on the KTP crystal length and was 11 cm^{-1} for our laser. This tuning was achieved by varying the crystal temperature from 20 to 30 °C. Fine tuning was performed by means of a piezoelectric element on which one of the resonator mirrors was mounted. The laser resonator had a very rigid construction which provided the high short-term radiation frequency stability ($\sim$ 10 kHz). The laser could be actively stabilised by the saturated absorption resonance in iodine and could be precisely locked in this way to the line centre. The study of the frequency stability with the help of two identical stabilised lasers showed that this stability during 200 s was no worse than 10^{-14}.

The source of probe radiation was a tunable external cavity diode laser. We used single-mode laser diodes (Polyus Research and Production Association) with the AR-coated output face (the output mirror reflection was $\sim$ 20 %) emitting at $\sim$ 980 nm. The typical threshold current and maximum output power were 40 mA and 50 mW, respectively. The external laser cavity is constructed in the autocollimation scheme and has the V-shaped configuration. A collimated beam behind a microscopic objective is incident on a mirror which directs it at the required diffraction angle on a diffraction grating. This configuration is chosen because a 1800 lines mm^{-1} diffraction grating that we use has the high diffraction efficiency (78.5 %) in the emission range of the laser in the first order for polarisation perpendicular to the gratings lines, while its efficiency for polarisation parallel to the grating lines is too low (10 %). If in the first case the zero diffraction order radiation, which amounts to 7 %, is used as the output radiation, the cavity proves to be underloaded and the output power is low. In the second case, feedback proves to be insufficient for stable lasing. In the given configuration, radiation is coupled out though the mirror and the cavity load can be easily optimised by selecting the transmission coefficient of the mirror. Another advantage of this scheme is that the output beam is not deflected during laser tuning. Tuning is performed by rotating a mirror mounted on a miniature adjustment head with adjustment screws with a thread pitch of 0.3 mm. The gating is fixed on a piezoelectric ceramics. The mirror transmission is 32 %.

At first glance a disadvantage of this scheme is that the output power is distributed among three beams leaving the cavity: the laser diode beam transmitted through the mirror, the beam transmitted through the mirror after first-order diffraction from the grating, and the beam zero-order diffraction beam. However, it became clear during experiments that this not a disadvantage because all the three beams are used in the working scheme. To avoid the deflection of the first-order diffraction beam transmitted through the mirror during tuning, the beam was directed on an additional steering mirror mounted on the movable part of the adjustment head. After reflection from this mirror, the beam propagates parallel to the main beam and is not deflected upon rotation of the adjustment head. The main beam in the spectrometer is directed to an absorption cell, while the second beam is intended for using in a scheme for precise frequency measurements. The zero-order diffraction beam is used for diagnostics: a part of radiation is delivered through a fibre to a wavemeter and the other – to an interferometer and to control the output power of the laser.

The continuous tuning of the laser was performed within the $\sim$ 5-GHz range by means of a piezoelectric element. The total tuning range at the 20 % excess of the excitation threshold was 30 nm (from 968 to 998 nm).

The scheme of the experimental setup shown in Fig. 2 includes in fact two laser spectrometers: a saturated absorption spectrometer and a three-level spectrometer itself. A cell with molecular iodine is common for both spectrometers. The absorption spectrometer is necessary for obtaining narrow saturated absorption resonances, which are used for frequency locking of a Nd : YAG laser. This spectrometer is built based on the traditional scheme [29]. Second harmonic radiation is collimated, propagates through a half-wave plate rotating the polarisation plane and is incident on a polariser. Here, the beam is split into two orthogonally polarised beams. The intensity of each of the beams depends on the direction of the polarisation plane at the polariser input and can be varied by rotating the half-wave plate. Then, the beams are directed toward each other by mirrors to the cell with iodine vapour. One of them has a high intensity and serves for saturation, while the other beam of intensity an order of magnitude lower is used for probing. When the second harmonic frequency is tuned to the centre of the Doppler absorption line, both beams interact with the same atoms. If the saturating beam is modulated by the amplitude, frequency or phase, this modulation is transferred to the probe beam due to nonlinear interaction. We used the phase modulation of the

saturating beam with the help of an electrooptical modulator (EOM) placed in the laser beam directed to the cell. The nonlinear interaction of the counterpropagating probe beam with the phase-modulated saturating beam in the cell leads to the phase modulation of the probe beam [30]. After propagation trough the cell, the probe beam is incident on the polariser P2 and is reflected from it on a photodiode. The modulated signal from the photodiode is fed to the phase detector of an automatic frequency control (AFC) system. During laser tuning, the probe beam modulation appears only near the Doppler line centre. The detected signal has the shape of the dispersion curve of width of a few megahertz. This signal can be used as the error signal to stabilise the laser frequency or to record the HFS of the absorption line.

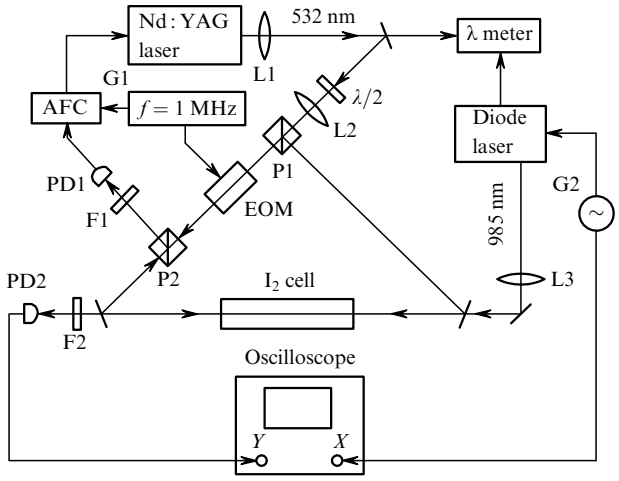

Figure 2. Scheme of the laser spectrometer: (AFC) automatic frequency control system; (EOM) electrooptical modulator; (PD1, PD2) photodetectors; (P1, P2) polarisers; (F1, F2) filters; (L1, L2, L3) lenses; (G1, G2) generators.

The optical scheme of the saturated absorption spectrometer considered above was used in the three-level laser spectrometer. It contained already most of the required elements of the spectrometer: the cell, the system for coupling the pump beam to the cell and the pump beam modulator. The mirrors used for coupling second-harmonic beams to the cell had the high transmission coefficient ($\sim 90\,\%$) at a wavelength of 985 nm and very low transmission ($\sim 0.1\,\%$) at 532 nm. Because of this, the diode laser beam was directed to the cell through one mirror and extracted from it through another mirror. In this case, the second mirror was used as a filter separating diode laser radiation from second harmonic radiation. The presence of two counterpropagating pump beams and the possibility of changing their intensities are very convenient in experiments because the shape and frequency of resonances in three-level spectroscopy depend on the mutual direction of the probe and pump beams.

In the first three-level spectroscopy experiments, we changed the pump beam focusing. To stabilise the laser frequency, the beam diameter in the cell was chosen to minimise the optical resonance width and, therefore, it was quite large (~ 1 mm) to reduce the influence of the time-of-flight broadening. It was very important, especially at the first stage of experiments, to maximise the useful signal in the spectrometer upon recording the optical resonance. For this purpose, the laser beam was focused to provide the minimum illuminated volume in the cell and, therefore, to obtain the maximum power density. Because the pump beam was astigmatic, it had two waists after focusing in vertical and horizontal planes separated by a distance of 6 cm and located in the middle part of the cell. The waist diameters were 0.5 and 0.38 mm. The probe beam was focused to provide the best overlap with the pump beam in the cell. The diode laser beam cross section had the elliptic shape with the axial ratio 1 : 4. To obtain the symmetric beam cross section, we used a two-prism expander providing the required beam expansion with the help of properly calculated prisms. The diameter of the beam waist located in the middle part of the cell was 0.45 mm.

The probe beam propagated through the cell was additionally filtered and incident on a PD 24-K silicon photodiode. A preliminarily amplified signal from the photodiode was fed to a phase detector and was then recorded with a digital oscilloscope. The pump radiation was modulated in phase by means of the EOM. The modulation frequency was 1 MHz at a modulation depth of 0.5, and the diode laser was tuned by applying a 50-Hz voltage to a piezoelectric element. When the optical scheme was carefully adjusted to minimise the noise caused by the parasitic optical feedback, optical resonances could be detected without modulation. In this case, the output signal of a photodetector was directly fed to an oscilloscope, and the amplification peak was observed by tuning the diode laser. The Nd : YAG and diode lasers were tuned to the required wavelength with the help of a wavemeter (Angstrem) providing the measurement accuracy no worse than 10^{-7}.

The glass cell with iodine vapour had a length of 30 cm. The vapour pressure was controlled by varying the temperature of a cooled side arm, which was stabilised with an electronic control system with an accuracy of 10 mK. Cooling was performed by means of a Peltier element.

4. Experimental results

The tuning range of the second harmonic of the pump laser was 22 cm^{-1} (from 18775 to 18797 cm^{-1}). In this range, 70 strong absorption lines of molecular iodine lie. By using data [1] and spectroscopic parameters of iodine molecules from [31, 32], we determined the vibrational and rotational quantum numbers for all transitions corresponding to these lines. All the transitions occur from the vibrational $v'' = 0$ level of the ground electronic $X\,^1\Sigma_g^+$ state to vibrational $v' = 32 - 37$ levels of the excited $B\,^3\Pi o_u^+$ state. The vibrational quantum numbers J'' of these transitions lie in the range from 48 to 146. Figure 1 presents the energy level diagram of an iodine molecule. After the determination of the quantum numbers of excited levels, we calculated the frequencies of emission transitions from these levels and selected transitions at the frequencies falling within the tuning range of the diode laser. These frequencies correspond to transitions to the vibrational levels of the ground electronic state with quantum numbers $v'' = 47$ and 48. The spectroscopic parameters that we used provided the calculation of the emission transition frequencies with the relative error no worse than 10^{-6}, which corresponds to ± 300 MHz. This accuracy is sufficient for tuning the diode

laser wavelength to the transition under study by using the wavemeter.

Figures 3–7 present the spectra of resonances recorded with the spectrometer. The resonances were excited at the $(J'' = 56, v'' = 0) \rightarrow (J' = 57, v' = 32)$ transition of iodine molecules and observed at the $(J' = 57, v' = 32) \rightarrow (J'' = 58, v'' = 48)$ transition. The wave number of the emission transition, calculated from data [31, 32], was 10152.386 cm^{-1}.

Figure 3 shows the HFS spectrum of the absorption line, which represents the output signal of the AFC phase detector recorded by slowly tuning the Nd:YAG laser. The commonly accepted notation of the HFS components is used. Table 1 presents frequency intervals between the components measured in paper [33]. Note that the HFS of many absorption lines falling within the tuning range of the Nd:YAG laser is very well studied and intervals between components are measured with an accuracy better than 10 kHz. The knowledge of the HFS of the absorption line considerably simplifies the assignment of the HFS components for the emission transitions. The matter is that the HFS parameters determining the structure of the spectrum depend to a greater extent on the rotational moment and only weakly on the internuclear distance in a molecule. As a result, in the three-level scheme, where two adjacent transitions differ only by the vibrational numbers of the ground state and, therefore, have close splitting parameters, the HFS structure of the emission line is very similar to that of the absorption line.

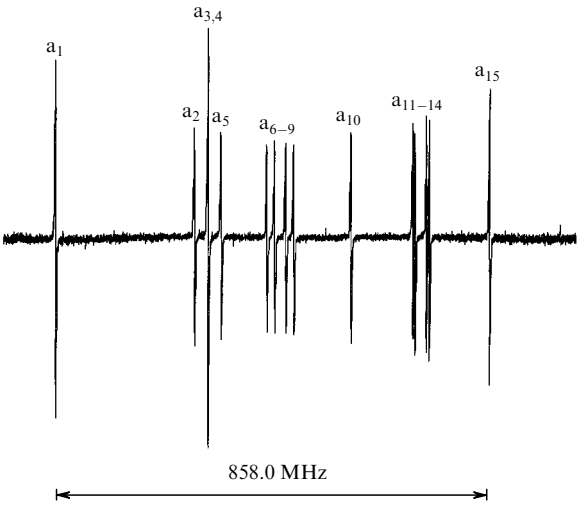

Figure 3. Hyperfine structure of the absorption line of the I_2 molecule at the 32–0 transition of the R(56) line recorded with a spectrometer by tuning the Nd:YAG laser.

By using the phase modulation of pump radiation, we recorded resonances at the emission transition as well. For this purpose, the probe beam propagating oppositely to the pump beam was introduced into the cell. The probe beam frequency was tuned with the help of the wavemeter to the calculated frequency of the emission transition. The output signal of the photodetector PD2 was fed to the AFC phase detector and then to an oscilloscope. The emission frequency of the Nd:YAG laser, which was preliminarily tuned approximately to the absorption line centre, was scanned by applying a 50-Hz voltage to a piezoelectric element. Usually, to record resonances, it was only necessary to tune slightly the diode laser frequency by varying a constant voltage applied to the piezoelectric element. Figure 4 shows emission resonances obtained by using modulation. These resonances, as absorption resonances, have the form of the dispersion dependence and can be used as an error signal to tune the diode laser frequency to the resonance centre. To provide the locking of the emission frequency of the stabilised laser to the transition frequency, the resonance should be located at the Doppler profile centre. This is achieved automatically if the pump frequency is locked to the saturated absorption resonance. Both resonances at the adjacent transitions appear simultaneously upon phase modulation of the pump beam in the presence of two counterpropagating pump waves in the cell. Thus, if the probe radiation frequency is stabilised simultaneously with the pump frequency, the probe radiation frequency will be locked to the transition frequency. To perform this, we have developed and are manufacturing now the appropriate equipment.

Table 1. Hyperfine splitting of the R(56) absorption line of the I_2 molecule at the 32–0 transition [33].

HFS component	Frequency shift/kHz
a_1	0
a_2	259698
a_3	285862
a_4	285862
a_5	311360
a_6	401480
a_7	416998
a_8	439626
a_{10}	571548
a_{11}	698045
a_{12}	702774
a_{13}	726031
a_{14}	732211
a_{15}	857960

The detailed study of the HFS of the emission transition was performed without modulation. The output signal of a photodetector was fed directly to an oscilloscope, and the alternate component of a signal appearing upon pumping at

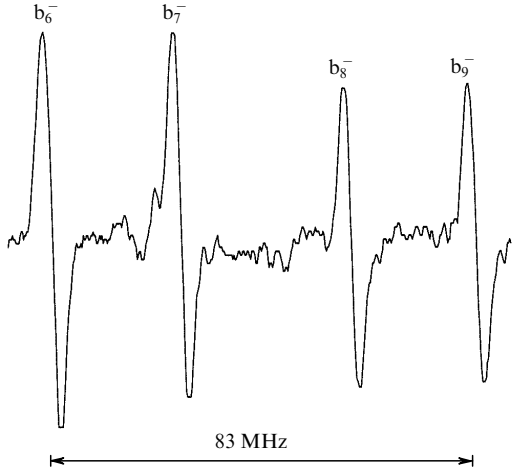

Figure 4. Hyperfine structure of the emission line of the I_2 molecule at the 48–32 transition of the P(58) line upon pumping at the 32–0 transition of the R(56) line. The tuning rate was 22 MHz ms^{-1}.

a fixed frequency during diode laser tuning was recorded. The resonances recorded in this way represent gain peaks produced by pumping. The gain at the adjacent transition can be determined from the amplitudes of the peaks. The gain is equal to the ratio of the alternate component of the signal to the part of the constant component caused by the probe radiation power transmitted through the cell.

Figure 5 presents the HFS spectrum of the emission transition for the case of unidirectional waves. A comparison of Figs 3 and 5 shows that the structures of both spectra are almost identical, taking into account that the spectrum in Fig. 5 does not contain the resonance corresponding to the component a_1. The spectrum in Fig. 5 has three resonances corresponding to components $a_2 - a_5$, the group of four resonances corresponding to components $a_6 - a_9$, two single resonances corresponding to a_{10} and a_{15}, and two resonances representing two unresolved doublets corresponding to components $a_{11} - a_{14}$. The resonances in Fig. 5 were numerated based on this correspondence. The resonance b_m corresponds to the transition having the common upper sublevel with the component a_m. The plus sign means that the resonances correspond to unidirectional waves. The spectrum was recorded by pumping at a frequency near the component a_{10} frequency. The entire emission transition spectrum can be also recorded by pumping at the frequency midway between the frequencies of components a_1 and a_{15}. In this case, the detuning from the Doppler profiles of these components will be 430 MHz. Calculations show that absorption at the Doppler profile wing at this detuning will be only $\sim 5\,\%$ of absorption at the profile centre. A weak signal appearing in this case can be recorded by increasing the pump power, thereby improving the signal-to-noise ratio. The frequency scale in Fig. 5 is determined from additional measurements, which will be described below. We see that frequency scales in Figs 3 and 5 are considerably different. This difference is explained by relation (8), from which it follows that frequency intervals between resonances in the case of unidirectional waves are smaller than intervals between the frequencies of corresponding transitions by the value $k_e/k_a\Delta\omega$. In our case, $k_e/k_a = 0.54$ and $\Delta\omega_{2.15} = 598$ MHz and, correspondingly, $k_e/k_a\Delta\omega_{2.15} = 323$ Hz. If frequency intervals between components of the absorption and emission lines were absolutely equal, i.e. $\Delta\omega_{2.15} = \Delta\Omega_{2.15}$, the interval between corresponding resonances would be 275 MHz, which insignificantly differs from the measured value 256 MHz.

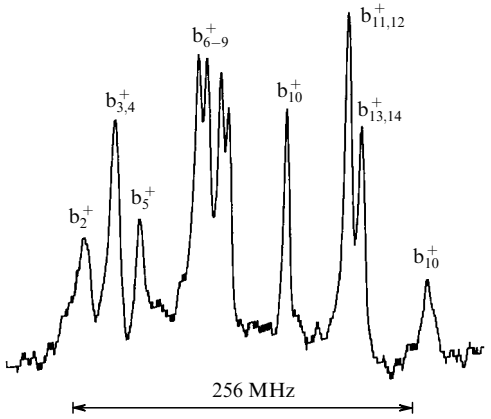

Figure 5. Hyperfine structure of the P(58) emission line of the I_2 molecule at the 48–32 transition upon pumping at the 32–0 transition of the R(56) line. The tuning rate was 66 MHz ms^{-1}.

Figure 6 presents a fragment of a spectrum recorded by pumping I_2 in the cell by two counterpropagating beams. The spectrum contains resonances which are typical both for counterpropagating and unidirectional waves. The plus and minus signs denote unidirectional and counterpropagating waves, respectively. To determine the type of the observed resonances, it is sufficient to block one of the pump beams. The spectra presented above were recorded by pumping at the frequency of the component a_{10}. The frequency of the Nd : YAG laser was not stabilised during the recording of spectra, and the accuracy of tuning to the centre of the component a_{10} was determined by observing resonances b^+_{10} and b^-_{10} of the emission transition. Upon tuning to the Doppler profile centre, the resonances merge to one, according to (6) and (7), and they are split upon detuning. One can see from the spectrum that, in accordance with (8) and (9), the frequency intervals between resonances excited by counterpropagating waves are almost three times larger than in the case of unidirectional waves. For this reason, the components b_{11} and b_{12}, as well as b_{13} and b_{14}, which are unresolved in the case of the unidirectional waves, become resolved upon pumping by counterpropagating waves. The part of the spectrum located from the low-frequency side of the component b_{10} was recorded similarly. However, when the entire spectrum was recorded at once, the recording quality was considerably worse because the extension of the tuning range reduced the signal-to-noise ratio due to the increase in the tuning rate.

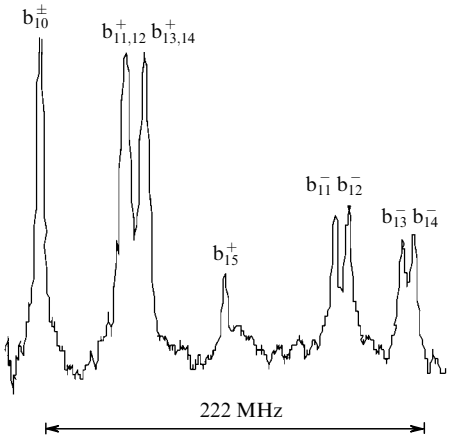

Figure 6. Hyperfine structure of the P(58) emission line of the I_2 molecule at the 48–32 transition upon pumping at the centre of the component a_{10} of the R(56) absorption line at the 32–0 transition. The tuning rate was 38 MHz ms^{-1}.

Spectra of the type presented in Fig. 6 were processed by using relations (10) and (11). The coordinates of resonances taken from the data obtained with a digital oscilloscope were introduced to the developed program, which calculated the frequency scale for each spectrum and frequency intervals between resonances and the HFS components of the emission transition. The scatter of frequency intervals calculated for different spectra was 5 %–7 %. This is explained by the fact that the frequency scale depends on the voltage across a piezoelectric element because of its

nonlinearity. Thus, this method can be used only for a rough determination of the frequency scale of the spectra. To improve the accuracy, it is necessary to increase considerably the linearity of the diode laser tuning. We plan in the future to measure accurately the frequency intervals by the heterodyne method.

The spectrum shown in Fig. 6 was recorded upon pumping by two counterpropagating waves with powers 4 and 3 mW, the probe radiation power was ~ 0.5 mW. The gain corresponding to the resonance b_{10} in Fig. 6 is 3×10^{-3}. This value corresponds to a total pump power of 7 mW because the resonance b_{10} is produced under the action of two counterpropagating waves. The iodine vapour pressure in the cell was 50 mTorr. At this pressure and a pump power of 3 mW, 70 % of the input power was absorbed. An increase in the I_2 vapour pressure in the cell did not result in a noticeable increase in the amplitude of resonances. This can be explained by the fact that the absorbed power and, hence, a total number of excited molecules increase only weakly with increasing pressure. In addition, the pressure broadening of lines reduces the amplitude of resonances.

Despite a relatively low pump power, we observed the dynamic Stark effect: as the tuning rate was decreased, a dip was observed at the centre of resonances for unidirectional waves. This is illustrated in Fig. 7, where the b_{10} resonances recorded for the counterpropagating and concurrent waves are presented. We determined the saturation value by measuring absorption in the cell at the pump power reduced by a factor of twenty. In this case, absorption increased from 70 % to 78%, which corresponds to the saturation parameter $I/I_0 = 0.28$, where I is the radiation intensity in the cell and I_0 is the saturation intensity.

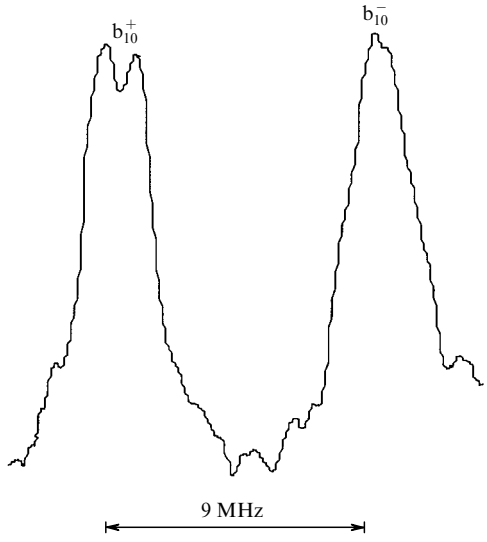

Figure 7. Resonance b_{10} recorded at a small detuning of the pump frequency from the centre of the Doppler profile of the component a_{10} and at a slower tuning. The tuning rate was 5 MHz ms^{-1}, pressure in the cell was 50 mTorr.

5. Conclusions

The experimental tests of the operation of the laser spectrometer developed in our study have shown that this spectrometer can be used for detail investigations of the HFS of emission lines. Resonances can be reliably recorded at comparatively low excitation powers (only 3–4 mW), which are more than an order of magnitude smaller than in the generation method. Note that the Franck–Condon coefficient, which is equal to 3.5×10^{-3} [32] for the transition under study, is smaller than the average value for this range and more than an order of magnitude smaller than that for transitions in the 1.3-μm region. A further improvement of the detection method will further reduce the required excitation power.

An important advantage of the spectrometer is that it allows one to record resonances simultaneously in absorption and emission upon the phase modulation of exciting radiation. The simultaneous stabilisation of frequencies of both lasers by these resonances should provide the frequency locking of a probe laser to the emission transition frequency. Thus, the HFS components of emission transitions can be used as frequency references to stabilise the radiation frequency of lasers with the expected frequency reproducibility no worse than 10^{-10}. By exciting molecules by our Nd:YAG laser, we can obtain about 5000 active emission transitions in the range between 0.8 and 1.34 μm. Therefore, taking the HFS into account, the number of frequency references will be $\sim 10^5$. It can be increased by several times by using other lasers for excitation, for example, the second harmonic of a Yb:YAG laser. Note that at present there are no references to stabilise the laser radiation frequency in the range from 0.8 to 1.3 μm. At the same time, a number of efficient tunable lasers are used for spectroscopy, communication, and metrology in this spectral range, which requires the stabilisation of their frequency.

We plan in the future to measure frequency intervals between the HFS components of emission lines by the heterodyne method and to determine the frequencies of individual HFS components by using a femtosecond synthesiser of optical frequencies. The precise measurement of emission transition frequencies will allow us to measure accurately the energies of high-lying vibrational–rotational levels of the ground electronic state of the iodine molecule and refine the shape of the potential curve of the ground state.

These data can be also used to determine more accurately the spectral emission parameters of I_2 molecules, which in turn will provide precise measurements of frequencies of any emission transitions. As a result, the emission spectrum can be used as the frequency scale in the range from 0.8 to 1.34 μm, by supplementing the frequency scale based on the absorption spectrum.

Acknowledgements. The authors thank A.V. Astapchuk for his help in calculations of the transition frequencies of molecular iodine and P.V. Travnikov for his help in experiments. This work was supported by the Russian Foundation for Basic Research (Grant Nos 05-02-1706 and 05-02-17854).

References

1. Gerstenkorn S., Luc P. *Atlas du spectre d'absorption de la molécule d'iode, 14000–15600 cm^{-1}, 15600–17600 cm^{-1}, 17500–20000 cm^{-1}* (91405 Orsay, France, Laboratoire Aime Cotton, CNRS II, 1977, 1977, 1978); Gerstenkorn S., Verges J., Chevillard J. *Atlas du spectre d'absorption de la molécule d'iode,*

11000 – 14000 cm^{-1} (91405 Orsay, France, Laboratoire Aime Cotton, CNRS II, 1982).
2. Sansonetti C.J. *J. Opt. Soc. Am. B*, **14**, 1913 (1997).
3. Velchev I., van Dierendonck R., Hogervorst W., Ubachs W. *J. Mol. Spectrosc.*, **187**, 21 (1998).
4. Xu S.C., van Dierendonck R., Hogervorst W., Ubachs W. *J. Mol. Spectrosc.*, **201**, 256 (2000).
5. Kato H. *Doppler-Free High Resolution Spectral Atlas of Odine Molecule* (Tokio, Japan Society for the Promotion of Science, 2000).
6. Bagayev S.N., Belkin A.M., Dychkov A.S., Farnosov S.A., Fateev N.V., Kolker D.B., Matyugin Yu.A., Okhapkin M.V., Pivtsov V.S., Zakharyash V.F., Zhmud V.A. *Proc. SPIE Int. Soc. Opt. Eng.*, **3736**, 310 (1999).
7. Bagayev S.N., Glushkov A.V., Dychkov A.S., Farnosov S.A., Fateev N.V., Karapuzikov A.I., Kolker D.B., Matyugin Yu.A. *Proc. 31st EGAS Conference* (Marseille, France, 1999) p. 131.
8. Bodermann B., Bëonsch G., Knëockel H., Nicolaus A., Tiemann E. *Metrologia*, **35**, 105 (1998).
9. Bodermann B., Klug M., Knëockel H., Tiemann E., Trebst T., Telle H.R. *Appl. Phys. B*, **67**, 95 (1998).
10. Bodermann B., Klug M., Winkelhoff U., Knëockel H., Tiemann E. *Eur. Phys. J. D*, **11**, 213 (2000).
11. Ye J., Robertsson L., Picard S., Ma L.-S., Hall J.L. *IEEE Trans. Instrum. Meas.*, **48**, 544 (1999).
12. Holzwarth R., Nevsky A.Yu., Zimmermann M., Udem Th., Hëansch T.W., von Zanthier J., Walther H., Knight J.G., Wadsworth W.J., Russell P.St.J., Skvortsov M.N., Bagayev S.N. *Appl. Phys. B*, **73**, 269 (2001).
13. Hong F.-L., Zhang Y., Ischikawa J., Onae A., Matsumoto H. *Opt. Commun.*, **212**, 89 (2002).
14. Knëockel H., Bodermann B., Tiemann E. *Eur. Phys. J. D*, **28**, 199 (2004).
15. Bodermann B., Knëockel H., Tiemann E. *Eur. Phys. J. D*, **19**, 31 (2002).
16. Byer R.L., Herbst R.L., Kildal H., Levenson M.D. *Appl. Phys. Lett.*, **20**, 463 (1972).
17. Koffend J.B., Field R.W. *J. Appl. Phys.*, **48**, 4468 (1977).
18. Wellegehausen B., Stephan K.H., Friede D., Welling H. *Opt. Commun.*, **23**, 157 (1977).
19. Koffend J.B., Goldstein S., Bacis R., Field R.W., Ezekiel S. *Phys. Rev. Lett.*, **41**, 1040 (1978).
20. Matyugn Yu.A., Ustinov G.N. *Kvantovaya Elektron.*, **6**, 2182 (1979) [*Sov. J. Quantum Electron.*, **9**, 1278 (1979)].
21. Barwood G.P., Gill P., Marx B.R. *Opt. Commun.*, **41**, 195 (1982).
22. Arie A., Schiller S., Gustafson E.K., Byer R.L. *Opt. Lett.*, **17**, 1204 (1992).
23. Klug M., Schulze K., Hinze U., Apolonskii A., Tiemann E., Wellegehausen B. *Opt. Commun.*, **184**, 215 (2000).
24. Ye J., Robertsson L., Picard S., Ma L-S., Hall J.L. *IEEE Trans. Instrum. Meas.*, **48**, 544 (1999).
25. Okhapkin M.V., Skvortsov M.N., Belkin A.M., Kvashnin N.L., Bagayev S.N. *Opt. Commun.*, **203**, 359 (2002).
26. Beterov I.M., Chebotaev V.P. *Progr. Quantum Electronics* (New York: Pergamon Press, 1974) Vol. 3, pt 1, p. 1.
27. Hackel P.R., Ezekiel S. *Phys. Rev. Lett.*, **42**, 1736 (1979).
28. Wellegehausen B. *IEEE J. Quantum Electron.*, **15,** 1108 (1979).
29. Eickhoff M.L., Hall J.L. *IEEE Trans. Instrum. Meas.*, **44**, 155 (1995).
30. Shirley J.H. *Opt. Lett.*, **7**, 537 (1982).
31. Gerstenkorn S., Luc P. *J. Physique*, **46**, 867 (1985).
32. Martin F., Bacis R., Churassy S., Verges J. *J. Mol. Spectrosc.*, **116**, 71 (1986).
33. Arie A., Byer R.L. *J. Opt. Soc. Am. B*, **10**, 1990 (1993).